

RINTC PROJECT: NONLINEAR DYNAMIC ANALYSES OF ITALIAN CODE-CONFORMING REINFORCED CONCRETE BUILDINGS FOR RISK OF COLLAPSE ASSESSMENT

**Guido Camata¹, Francesca Celano², Maria Teresa De Risi², Paolo Franchin³,
Gennaro Magliulo², Vincenzo Manfredi⁴, Angelo Masi⁴, Fabrizio Mollaioli³, Fabrizio Noto³,
Paolo Ricci², Enrico Spacone¹, Marco Terrenzi¹, Gerardo Verderame²**

¹ University G. d'Annunzio of Chieti-Pescara
Dept. of Engineering and Geology, viale Pindaro 42, 65127 Pescara, Italy
e-mail: guido.camata@unich.it, espacone@unich.it, marco.terrenzi@unich.it

² University of Naples Federico II
Dept. of Structures for Engineering and Architecture, via Gramsci 53, 00197 Rome, Italy
e-mail: gennaro.magliulo@unina.it, verderam@unina.it, fr.celano@gmail.com,
mariateresa.derisi@unina.it, paolo.ricci@unina.it

³ Sapienza University of Rome
Dept. of Structural and Geotechnical Engineering, via Claudio 21, 80125 Naples, Italy
e-mail: paolo.franchin@uniroma1.it, fabrizio.mollaioli@uniroma1.it, fabrizio.noto@gmail.com

⁴ University of Basilicata
Dept. of Structures, Geotechnics and Geology, 85100 Potenza, Italy
e-mail: angelo.masi@unibas.it, enzo.manfredi@alice.it

Keywords: reinforced concrete, nonlinear static and dynamic analyses, lumped plasticity models, infill models, multi-stripe analyses, risk assessment.

Abstract. *This paper reports on the results of an ongoing Research Project aimed at computing the risk of collapse in code-conforming new Italian buildings. A companion paper describe the overall Research Project ([11]), funded by the Italian Civil Protection Department (DPC), its different areas of application (reinforced concrete, masonry, steel buildings, etc), the overall seismic risk calculation procedure and the ground motion selection process for the recorded ground motions used for the multi-stripe analyses. This paper deals with different classes of reinforced concrete buildings (namely 3-, 6- and 9- story high moment resisting frame) designed in cities with increasing seismic hazard. For the sake of brevity, only the results of 6-story buildings are reported. First, the paper describes the geometry, material characteristics and main design properties of the buildings, including their elastic dynamic properties. Three different configurations are considered: Bare Frame (BF), Infill Frame (IF) and Pilotis Frame (PF, that is a building with infills at all levels except for the ground level). Design of the first two configurations is identical, while the PF requires an increase in the design forces at the ground level. Second, the paper introduces the nonlinear models used for the nonlinear analyses: lumped plasticity models for beams and columns, strut and tie models for the infills. Since the buildings are designed according to capacity design principles, the nonlinear behaviors of beams and columns in shear and of beam-column joints are not considered. Pushover analyses are used to estimate the EDP (top floor displacement) value used for the definition of the collapse limit state. Finally, the results of the multi-stripe analyses are presented for ten different ground motion intensities.*

1 INTRODUCTION

Three sets of 3, 6 and 9-story moment-resisting frame buildings were designed. The buildings are all intended for residential use and are characterized by regularity in plan and elevation. The ground level is 3.4m high, all other stories are 3.05m high. The staircase is designed with knee beams. All buildings have identical floor plans (floor beams and floor slabs), the only differences being in the column dimensions and reinforcement. For length reasons, this paper presents the 6-story buildings only.

Design of the RC buildings followed the Italian NTC 2008 [14] design code. All buildings were designed in low ductility class using Response Spectrum Analysis. The buildings are on soil type C. The structures are moment resisting frames assumed fixed at the base.

The minimum column size is 35 cm. Figure 1a shows the typical structural plan, where the fixed reference grid is highlighted. The arrows indicate the orientation of the one way slabs. The outer beams are all deep, while all internal beams are flat (for this reason the building automatically falls into the low ductility category of NTC 2008). The slab thickness is 25cm. Figure 1b shows the beam details. Three different infill configurations are considered, as summarized in Figure 2: Bare Frame (BF), Infill Frame (IF), Pilotis Frame (PF).

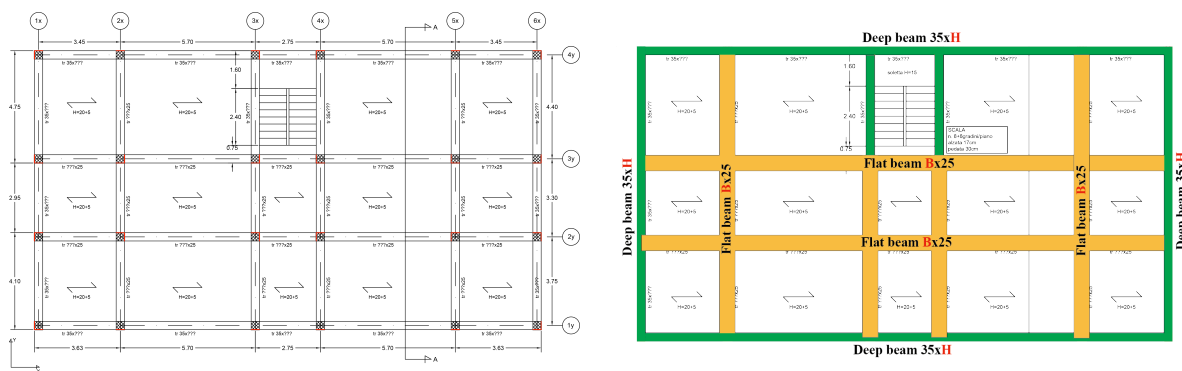


Figure 1: a) floor plan with fixed reference grid and one way slab orientation
b) beam types

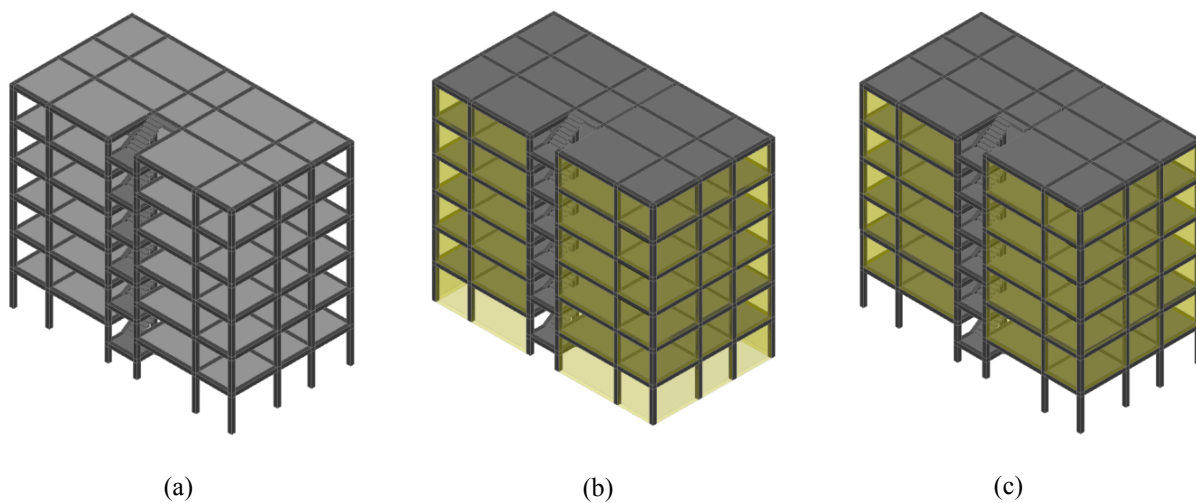


Figure 2: 6-story buildings: bare frame BF (a); infill frame IF (b); pilotis frame PF (c)

From the design viewpoint, BF and IF are identical. For PF buildings, the Italian NTC 2008 prescribes that all actions be increased by 40% for the vertical elements in stories with an infill reduction (base floor in PF). Finally, concrete C28/35 and B450C steel were used.

The elastic response spectra on bedrock for the five sites are shown in Figure 3. The seismic design of the RC buildings was performed by means of a modal response spectrum analysis. The buildings' behavior factor was $q=3.9$. All buildings were designed to be regular in plan and elevation.

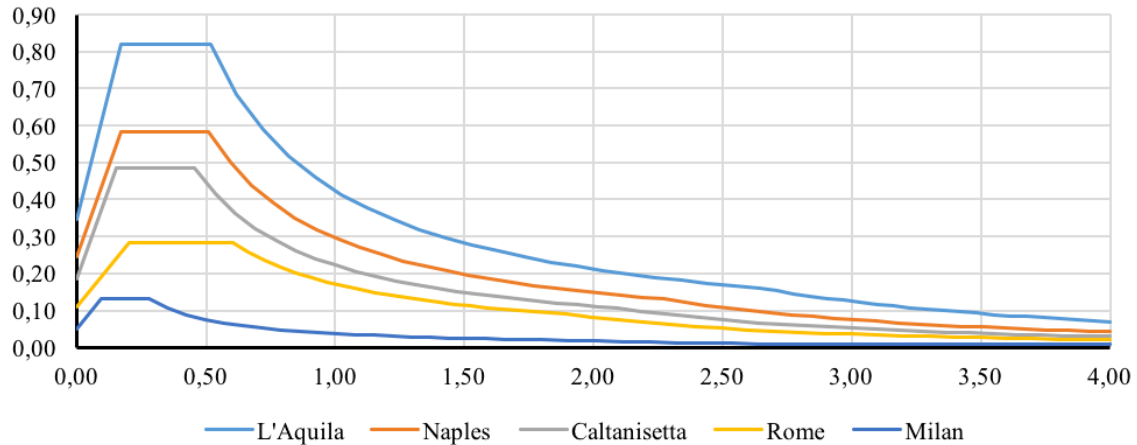


Figure 3: Horizontal elastic response spectra for 475 years return period design earthquake at five building sites (soil type C)

Table 1 and Table 2 summarize the main design data for the five buildings considered.

City	T_x [s]	M_x [%]	T_y [s]	M_y [%]
Milan	1.66	75	1.42	83
Caltanissetta	1.09	83	0.90	83
Rome	1.04	81	0.97	82
Naples	0.88	82	0.80	83
L'Aquila	0.90	78	0.79	77

Table 1: Summary of modal parameters for 6-story buildings

City	Average floor seismic weight [kN/m ²]	$\Sigma A_{col}/A_{floor}$ [%]	$\rho_{b_deep,1,m}$ [%]	$\rho_{b_flat,1,m}$ [%]	$\rho_{c,1,m}$ [%]
Milan	11.25	1.16	0.43	0.34	1.37
Caltanissetta	11.40	1.57	0.89	1.10	1.53
Rome	10.93	1.60	0.96	0.93	1.29
Naples	12.94	2.17	0.72	0.84	1.46
L'Aquila	13.03	3.10	1.51	1.23	1.08 ÷ 1.41

Table 2: Summary of design data for all 6-story buildings

The following symbols are used:

T_x, M_x = fundamental period in the x dir. and corresponding mass participation factor;

T_y, M_y = fundamental period in the y dir. and corresponding mass participation factor;

$\Sigma A_{col}/A_{floor}$ = total column area at the ground floor/total floor area;

$\rho_{b_deep,1,m}$ = average deep beams' longitudinal steel ratio;

$\rho_{b_flat,1,m}$ = average flat beams' longitudinal steel ratio;

$\rho_{c,1,m}$ = average base floor columns' steel ratio.

The column sizes mainly derive from pre-sizing based on the assumed maximum normalized axial load, particularly for sites with low seismic hazard. In most cases the amount of reinforcement is given by the minimum reinforcement requirements of NTC 2008 [14], thus reducing the differences between IF/BF and PF buildings to a minimum (they are, in some cases, identical). The staircase knee beams experience high tension/compression excursions, pointing to possible numerical issues in the nonlinear analyses. The column area increases with the site seismic intensity, while the reinforcement ratio stays almost constant, due to the minimum reinforcement requirements in the design code.

2 MODELLING ISSUES AND MODELLING STRATEGIES

Because the buildings were designed using capacity design principles, only nonlinearities in the beams, columns (flexural only) and masonry infills were considered. The computational platform was OpenSees [13]. The sizes of the buildings and the number of analyses to be carried out for the multiple-stripe analyses (10 intensity levels with 20 ground motions per stripe) called for pragmatic choices in the structure modelling.

The model selected for the section flexural behavior is the well-tested model by Ibarra et al. [9, 10], in its most recent OpenSees implementation (modIMKmodel). The model has already been used in a similar setting, i.e. for the probabilistic seismic performance assessment of both existing and code-conforming (plane) frame structures [8, 12].

The model is defined through seven parameters in each loading direction, as shown in Figure 4. This model can be used to describe the moment-rotation relationship, independently of axial load and in a single plane of flexure. The main advantages of this model are its computational efficiency, its computational robustness, its capability of describing the degrading response of the sections, the availability of predictive equations for the IMK model parameters from previous work [7].

As for the elements, a Tcl/Tk procedure was used to generate internal nodes coincident with the i and j nodes of each member, and *zeroLength* elements were used to describe inelastic response confined in these end sections. The internal portion was modelled with an elastic frame element. This way, there is no need for element iterations (needed in force-based elements), thus leaving complete control over the iterations to the global convergence algorithm, by employing nodes with global degrees of freedom (labeled 'internal' in Figure 4) for the plastic hinges too.

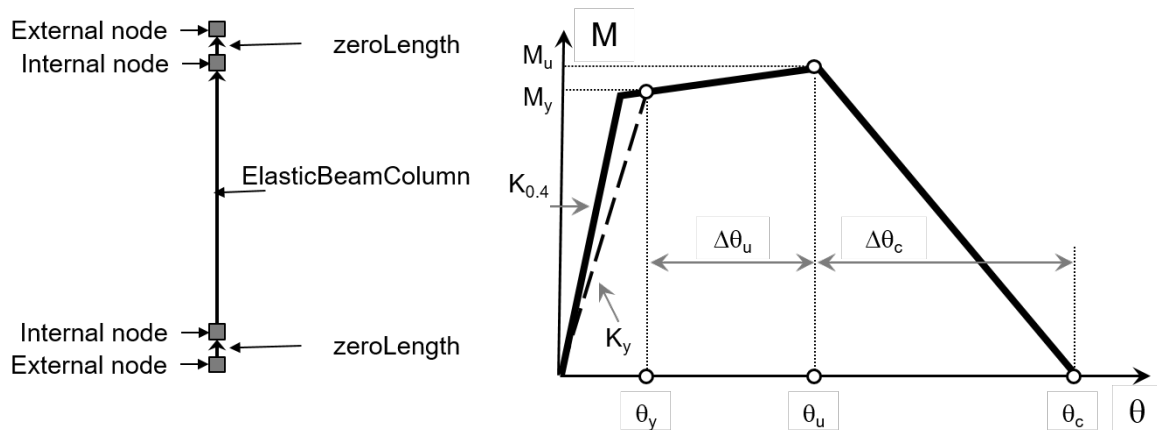


Figure 4: Frame model used for beams and columns: assembly of *zeroLength* inelastic elements and elastic-BeamColumn element (left), moment-rotation law (backbone) according to the Ibarra et al [10] model (right)

For each plane of flexure, the following parameters were determined for the member-level moment-rotation properties:

$$\Delta\theta_u = 0.13(1 + 0.55a_{sl})(0.13)^v(0.02 + 40\rho_{sh})^{0.65}(0.57)^{0.01f_c} \quad (1)$$

$$\Delta\theta_c = 0.76(0.31)^v(0.02 + 40\rho_{sh})^{1.02} \leq 0.10 \quad (2)$$

$$k_{0.4} = 0.17 + 1.61v \begin{cases} \geq 0.35 \\ \leq 0.80 \end{cases}, \quad K_{0.4} = k_{0.4} \frac{3EI_0}{L_v} \quad (3)$$

$$k_y = 0.065 + 1.05v \begin{cases} \geq 0.20 \\ \leq 0.60 \end{cases}, \quad K_y = k_y \frac{3EI_0}{L_v} \quad (4)$$

$$\alpha_y = \frac{M_u}{M_y} = 1.25(0.89)^v(0.91)^{0.01f_c} \quad (5)$$

$$\gamma = \frac{E_t}{M_y \theta_y} = 170.7(0.27)^v(0.10)^{s/d} \quad (6)$$

Since the elements are in series, the moment thresholds of the inelastic sections are the same as those of the member, while deformation thresholds are a function of the stiffness ratio $n = k_s/k_e$, where the “s” and “e” subscripts denote the section and the elastic element, respectively (Ibarra and Krawinkler [9] – Appendix B) [9, 10]. It can be shown that: $k_s = (n+1)k_m$, $\Delta\theta_m = \Delta\theta_s + \Delta\theta_e$ and $\Delta\theta_s = \Delta\theta_m(1/n+1)$.

Modeling of the stairwell structure requires particular care. The stairwell structure comprises inclined beams and cantilever steps. The large axial force variations in the inclined beams induce large shear forces in the adjoining members. The phenomenological IMK model was modified for the staircase beams. The stiffness of the axial degree of freedom of the internal elasticBeamColumn element was set to zero, while adding an inelastic truss element in parallel. The latter is assigned a non-symmetric elastic-plastic constitutive law with limits proportional to $A_s f_y$ in tension and $A_c f_c$ in compression, respectively.

As for the masonry infills, their contribution was modeled through an equivalent strut acting in compression only (Figure 5). The equivalent diagonal strut is a consolidated engineering model for infilled frames that is also proposed for the design of infilled frames by several codes.

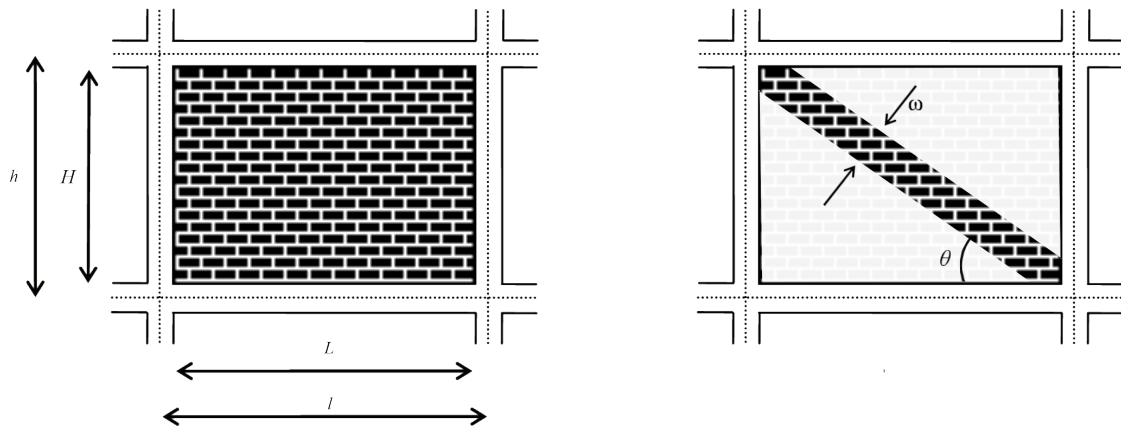


Figure 5: Diagonal strut model

The Decanini et al. model [2, 3, 4] was selected for modeling the struts. The infill panel strength was simulated by a fictitious failure compressive stress σ_{br} , taking into account the different failure modes occurring both in laboratory tests and in real structures subjected to seismic action. Four basic failure modes are considered, with the corresponding equivalent failure compressive stresses: (a) diagonal tension, $\sigma_{br(1)}$; (b) sliding shear along horizontal joints, $\sigma_{br(2)}$; (c) crushing in the corners in contact with the frame, $\sigma_{br(3)}$; (d) diagonal compression, $\sigma_{br(4)}$.

$$\sigma_{br(1)} = \frac{0.6\tau_{m0} + 0.3\sigma_o}{\omega / d} \quad (7)$$

$$\sigma_{br(2)} = \frac{(1.2\sin\theta + 0.45\cos\theta)u + 0.3\sigma_o}{\omega / d} \quad (8)$$

$$\sigma_{br(3)} = \frac{(1.12\sin\theta \cdot \cos\theta)}{K_1(\lambda h)^{-0.12} + K_2(\lambda h)^{-0.88}} \sigma_{m0} \quad (9)$$

$$\sigma_{br(4)} = \frac{1.16\sigma_{m0} \tan\theta}{K_1 + K_2\lambda h} \quad (10)$$

where σ_{m0} is the vertical compression strength measured on masonry specimens, τ_{m0} is the shear strength measured with the diagonal compression test, u is the sliding strength in the joints, and σ_o is the vertical stress due to gravitational loads. The ultimate lateral strength H_{mfc} of the strut was selected as the minimum value among the capacities associated with the four in-plane failure modes.

$$H_{mfc} = \sigma_{\min} e \omega \cos\theta \quad (11)$$

where e is the panel thickness. The ultimate lateral strength H_{mfc} was incremented by a factor estimated at 1.18 to obtain the median value of the available database. The width of the strut, ω , is introduced by means of the relative stiffness parameter λh proposed by Stafford-Smith [15] and by two constants K_1 and K_2 calibrated on the basis of experimental tests:

$$\omega = \left(\frac{K_1}{\lambda h} + K_2 \right) d \quad (12)$$

$$\lambda h = \sqrt[4]{\frac{E_m e \sin(2\theta)}{4E_c I h_m}} h \quad (13)$$

where λh is a non-dimensional parameter that depends on the geometric and mechanical characteristics of the frame-infill system, K_1 and K_2 are coefficients that change according to λh , and d is the length of the equivalent strut (Table 3).

	K_1	K_2
$\lambda h \leq 3.14$	1.3	-0.178
$3.14 \leq \lambda h \leq 7.85$	0.707	0.01
$\lambda h \geq 7.85$	0.47	0.04

Table 3: Coefficients K_1 and K_2

E_m is the elastic equivalent modulus corresponding to the complete cracking stage of the infill, E_c is the elastic modulus of concrete, t is the slope of the strut to the respect of the horizontal axis, e is the thickness of the masonry panel, h is the story height, h_m is the height of the masonry panel, I is moment of inertia of the columns.

The stiffness of the equivalent strut K_{mfc} at complete cracking stage is given by the following relation:

$$K_{mfc} = \frac{E_m e \omega}{d} \cos^2 \theta \quad (14)$$

The skeleton curve of the lateral force-displacement (H_m-u) relationship includes the the four branches shown in Figure 6: initial elastic uncracked, post-cracking, descending branch following the maximum strength H_{mfc} , zero strength following the residual displacement u_r .

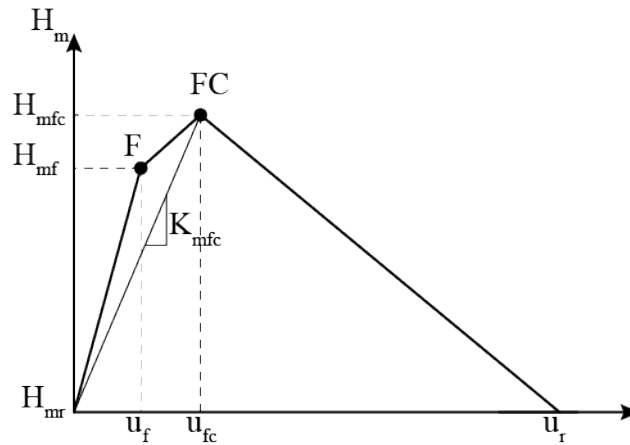


Figure 6: Backbone curve for the equivalent strut model

The effects of the openings were accounted for through reduction factors [1, 4, 15]. The force and drift values of the main points of the infills' backbone curves are reported in Figure 7. The infills were modeled in Opensees using the Concrete01 model.

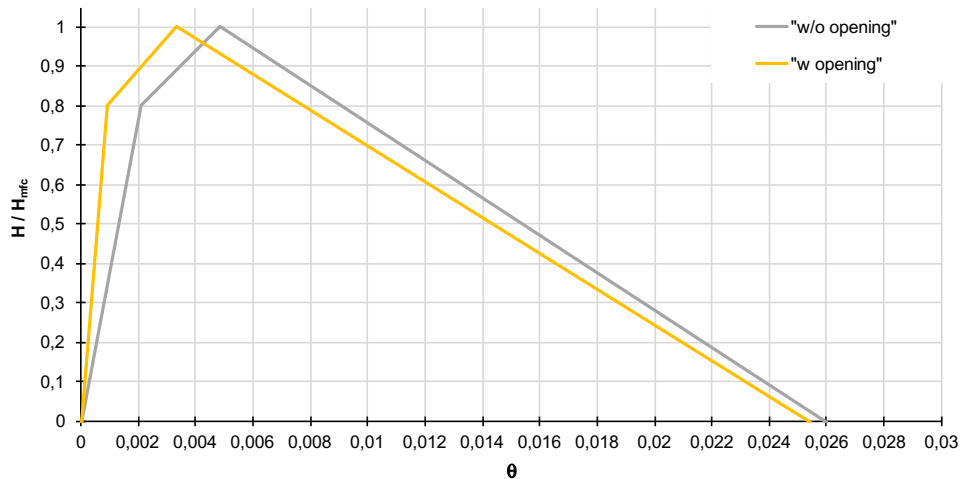


Figure 7: Backbone curve

3 RESULTS OF NONLINEAR DYNAMIC TIME HISTORY ANALYSES

The identification of global collapse through a numerical response analysis is not a trivial task. The buildings analyzed in this project are code-conforming, therefore no defective collapse modes should be activated. This implies that a purely global, state-evolutionary approach could be more reliably adopted. It was pragmatically chosen to employ a global, simplified collapse criterion based on a global capacity obtained from pushover analyses. Criticisms of this choice are known [5, 17], since a single capacity value, related to the collapse mechanism occurring in the pushover analysis, is adopted, rather than motion-specific values.

The adopted criterion is therefore an approximate one and capacity is defined as the value of drift (IDR or RDR can be used indifferently for these buildings) at 50% decrease in base shear on the negative slope (Figure 8). This value is preferred since it is easier to identify on the pushover curves and because it is lower than the monotonic value of displacement at zero base shear, and thus ideally closer to a generic ‘cyclic’ value of displacement at zero base shear.

Two values are determined, one in the X and the other in the Y direction (maximum absolute value), and the D/C ratio is reported independently in both directions.

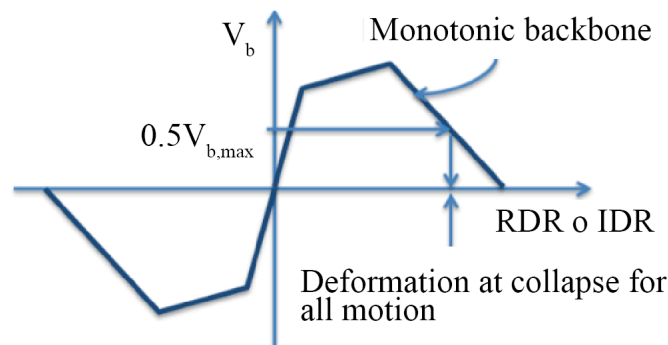


Figure 8: Collapse criteria: approximate approach based on displacement threshold from pushover analysis

Results of the analyses are summarized in terms of D/C ratios (largest over X and Y of top displacement demand -absolute value- to capacity). Before showing the results of the response-history analyses, the following figures present results of the nonlinear static pushovers, used to establish roof displacement thresholds at collapse. Differences mainly arise from design, where in addition to different seismicity, each research unit entrusted with designing the buildings at a single site, made slightly different (but reasonable) design decision.

Figure 9 and Figure 10 report the pushover results for the two main load shapes (modal and uniform), for the three different 6-story building configurations (BF, IF and PF) and for the two principal directions X and Y. It is quite clear that the curves for the three lower seismicity sites tend to lump in one group, and this is especially true for the BF configuration. The latter is also the one where differences can only be tracked to RC members and initial design. For these sites the minimum design requirements play an important role and thus the differences between the buildings vanish. At the other end of the spectrum, the pushover curves for the Naples and L'Aquila sites reflect the higher demands due to the higher seismic hazard. In the IF and PF pushover curves, the higher strength derives from the added shear carried by the infills. When the infills fail, a shear drop is evident in the pushover curves.

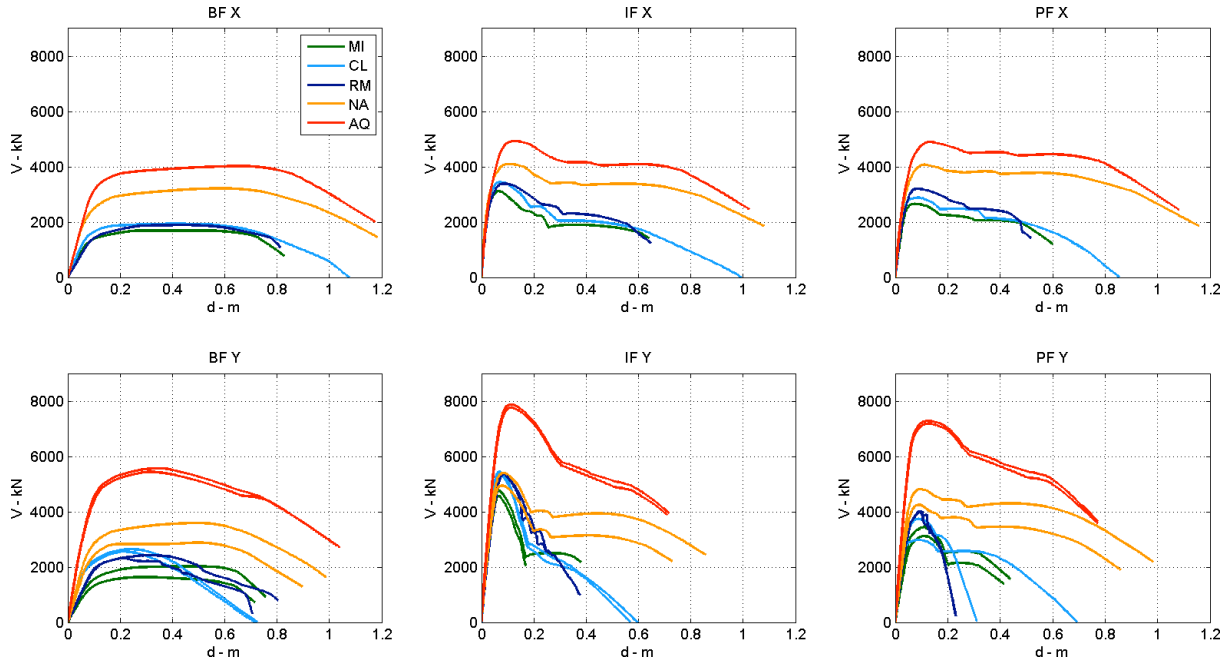


Figure 9: Modal pushover results in the X (top row) and Y (bottom row) directions, for the three configurations (BF, IF and PF from left to right).

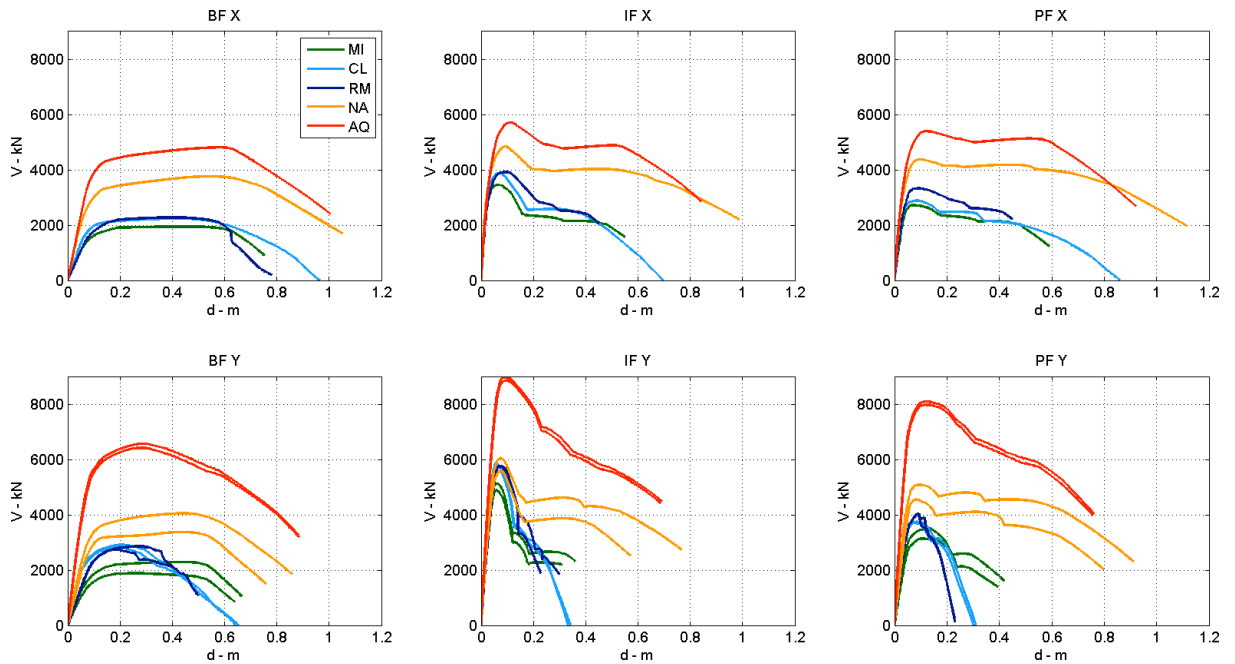


Figure 10: Uniform pushover results in the X (top row) and Y (bottom row) directions, for the three configurations (BF, IF and PF from left to right).

Finally, Figure 11 reports the D/C ratios (in terms of top floor displacement) for all buildings and all sites computed through nonlinear time history analyses at the ten selected intensity levels (multiple stripe analysis).

Results indicate that in general the D/C ratios are much lower than 1.0, except for the L'Aquila building for a 10^5 years return period (stripe 10). Also, the D/C ratios increase for buildings in sites of higher seismic intensity. In summary, input differences justifying the observed output should be traceable to:

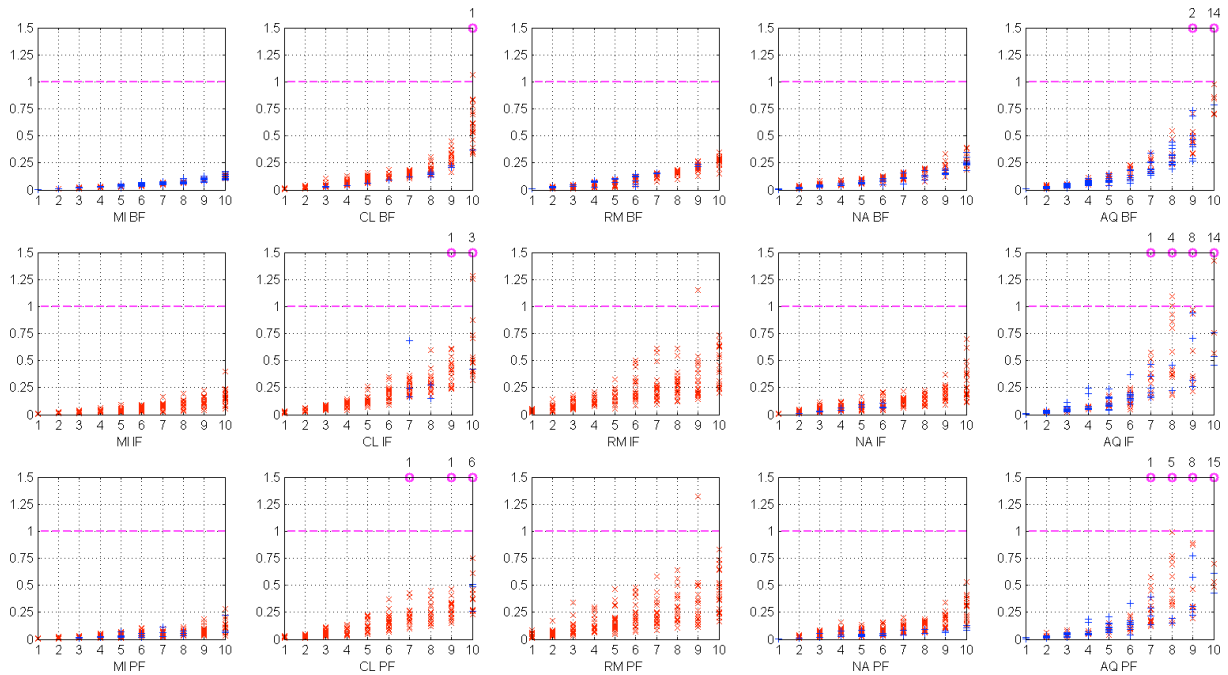


Figure 11: Collapse Limit State: D/C ratios for 6-Story buildings and sites: BF, IF and PF on the top, middle and bottom row, respectively. The figure reports on each intensity level the number of collapses (above magenta dots). D/C ratios in the x and y directions are indicated in red blue, respectively.

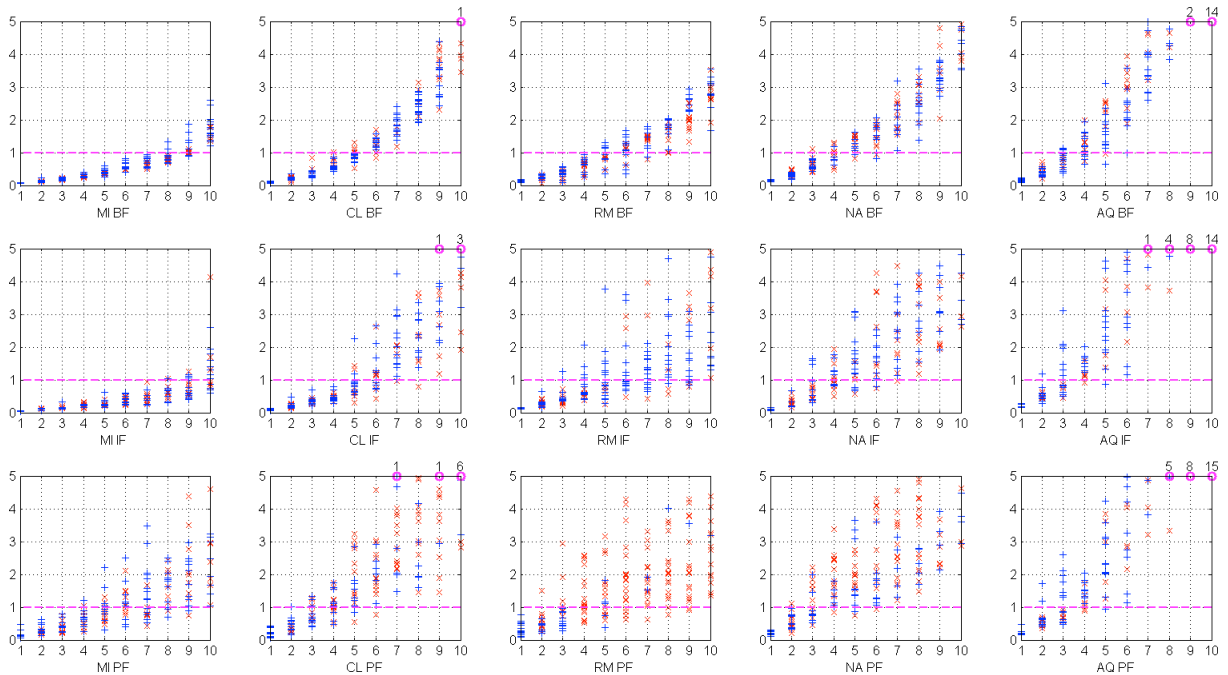


Figure 12: Damage Limit State: D/C ratios for 6-Story buildings and sites: BF, IF and PF on the top, middle and bottom row, respectively. The figure reports on each intensity levels the number of collapses (above magenta dots). D/C ratios in the x and y directions are indicated in red blue, respectively.

- seismic design intensity
- fundamental period and conditioning IM
- prevalent direction of strong bending axis in rectangular cross-sections
- reinforcement ratios and columns' concrete cross-section area

- effect of percent reduction in masonry infill strength as a function of openings in each direction

The Damage Limit State is defined in NTC2008 as the limit state where “the structure, including structural and nonstructural elements, and machines relevant to its functions, exhibit damage that does not expose its occupants to any risk, and that does not compromise the strength and stiffness of the structure with respect of the vertical and horizontal loads. The structure is immediately usable even if some machineries are not fully operational.” Based on the above definitions, Italian design guidelines define InterStory Drift Ratios (IDRs) for existing buildings: if the model includes the infills, $IDR \leq 0.003$ (IF and PF cases), in the Bare Frame case $IDR \leq 0.005$.

Figure 12 shows that the DLS is reached after the first few stripes. This is in line with the design procedure: the DLS is checked for an earthquake intensity roughly corresponding to the secondo stripe.

4 CONCLUSIONS

This paper presents the results of an ongoing project ([11]) on the implicit risk of seismic collapse (and damage) of buildings designed according to the current Italian design code NTC2008. The paper focuses on a set of 6-story reinforced concrete buildings designed in five sites of increasing seismic hazard. Simplified models were used to minimize the computational times and non-convergence issues. Since the buildings were designed following capacity design principles, the main modeling issues concern the flexural failures in beams and columns and the infill models. Definitions of collapse and damage limit states are discussed. The results from multiple-stripe analyses (20 NLTHA for 10 hazard levels) show that the only buildings showing collapse are those in L'Aquila (the site with the highest hazard level) and only for the last stripes corresponding to extremely long return periods. On the other hand, at the damage limit state, the analyses show that the damage limits are reached starting with the second or third stripe, that roughly correspond with the earthquake return period used for the DLS design. The project plans to extend the study to 3- and 9- story code-conforming RC frame buildings.

ACKNOWLEDGEMENTS

The authors would like to acknowledge the financial support of the Italian Civil Protection Department, ReLUIS project 2014-2018 (<http://www.reluis.it/>).

REFERENCES

- [1] Cardone, D., Perrone, G., Developing fragility curves and loss functions for masonry infill walls. *Earthquakes and Structures*, Vol. 9, No. 1, 257-279, 2015.
- [2] Decanini L.D., Fantin G.E., *Modelos simplificados de la mamposteria incluida en porticos. Caracteristicas de rigidez y resistencia lateral en estado limite*, Jornadas Argentinas de Ingenieria Estructural, Buenos Aires, Argentina, 1986, Vol.2, pp.817-836 (in Spanish), 1986.
- [3] Decanini, L., Mollaioli, F., Mura, A., Saragoni R., Seismic performance of masonry infilled R/C frames, *Proc.13th WCEE, Paper 165, Vancouver, B.C., Canada*, August 1-6, 2004.

-
- [4] Decanini L., Liberatore L., Mollaioli F. , *Strength and stiffness reduction factors for infilled frames with openings*, Earthquake Engineering and Engineering Vibration, **13**(3): 437-454, September, 2014.
 - [5] Goulet, C. A., Haselton, C. B., Mitrani-Reiser, J., Beck, J. L., Deierlein, G. G., Porter, K. A., & Stewart, J. P., *Evaluation of the seismic performance of a code-conforming reinforced-concrete frame building—from seismic hazard to collapse safety and economic losses*. Earthquake Engineering & Structural Dynamics, 36(13), 1973-1997, 2007.
 - [6] Haselton, C.B., Liel, A.B., Taylor Lange, S. & Deierlein, G.G., *Beam-Column Element Model Calibrated for Predicting Flexural Response Leading to Global Collapse of RC Frame Buildings*, PEER report 2007/03, 2008.
 - [7] Haselton, C. B., Liel, A. B., & Deierlein, G. G., Simulating structural collapse due to earthquakes: model idealization, model calibration, and numerical solution algorithms. *Computational Methods in Structural Dynamics and Earthquake Engineering (COMPdyn)*, 2009.
 - [8] Haselton, C. B., Liel, A. B., Deierlein, G. G., Dean, B. S., & Chou, J. H., *Seismic collapse safety of reinforced concrete buildings. I: Assessment of ductile moment frames*. Journal of Structural Engineering, 137(4), 481-491, 2010.
 - [9] Ibarra, L. F., & Krawinkler, H., *Global collapse of frame structures under seismic excitations*. Rep. No. TB 152, The John A. Blume Earthquake Engineering Center, 2005.
 - [10] Ibarra, L. F., Medina, R. A., & Krawinkler, H., *Hysteretic models that incorporate strength and stiffness deterioration*. Earthquake engineering & structural dynamics, 34(12), 1489-1511, 2005.
 - [11] I. Iervolino, A. Spillatura, P. Bazzurro, *RINTC Project - Assessing the (implicit) seismic risk of code-conforming structures in Italy*. COMPdyn 2017 - 6th ECCOMAS Thematic Conference on Computational Methods in Structural Dynamics and Earthquake Engineering M. Papadrakakis, M. Fragiadakis (eds.) Rhodes Island, Greece, 15–17 June 2017.
 - [12] Liel, A. B., Haselton, C. B., & Deierlein, G. G., *Seismic collapse safety of reinforced concrete buildings. II: Comparative assessment of nonductile and ductile moment frames*. Journal of Structural Engineering, 137(4), 492-502, 2010.
 - [13] McKenna, F. (2011) “OpenSees: a framework for earthquake engineering simulation”, Computing in Science & Engineering 13.4 (2011): 58-66 (<http://opensees.berkeley.edu>).
 - [14] NTC 2008, Norme Tecniche per le Costruzioni, Decreto ministeriale del 14 gennaio 2008, in Italian (Italian Building Code, 2008).
 - [15] Sassun, K., Sullivan, T. J., Morandi, P., Cardone, D., *Characterising the in-plane seismic performance of infill masonry*. Bulletin of the New Zealand Society for Earthquake Engineering, Vol. 49, No. 1, 100-117, 2016.
 - [16] Stafford Smith, B., *Lateral stiffness of infilled frames*, Journal of Structural Division, ASCE, Vol. 88, No. ST 6, pp 183-199, 1963.
 - [17] Villaverde, R., *Methods to assess the seismic collapse capacity of building structures: State of the art*. Journal of Structural Engineering, 133(1), 57-66, 2007.